Steel and Composite Structures, *Vol. 23, No. 6 (2017) 669-682*
DOI: https://doi.org/10.12989/scs.2017.23.6.669

Analysis of circular steel tube confined UHPC stub columns

An Le Hoang* and Ekkehard Fehling [a]

Faculty of Civil and Environmental Engineering, Institute of Structural Engineering, University of Kassel, Kurt-Wolters-Straße 3, 34125, Kassel, Germany

(*Received June 13, 2016, Revised January 24, 2017, Accepted February 20, 2017*)

Abstract. The use of ultra high performance concrete (UHPC) in composite columns offers numerous structural benefits, and has received recent research attention. However, the information regarding the behavior of steel tube confined concrete (STCC) columns employing UHPC has been extremely limited. Thus, this paper presents an overview of previous experimental studies on circular STCC columns with taking into account various concrete strengths to point out their distinctive features. The effect of the confinement factor and the diameter to thickness ratio on both strength and ductility in circular STCC columns employing UHPC was investigated. The applicability of current design codes such as EC4, AISC, AIJ and some available analytical models for concrete confined by steel tube was also validated by the comparison of ultimate loads between the prediction and the test results of Schneider (2006) and Xiong (2012). To predict the stress-strain curves for confined UHPC in circular STCC stub columns, a simplified model was proposed and verified by the comparison with experimental stress-strain curves.

Keywords: UHPC; STCC columns; confinement factor; strength; ductility; concrete filled steel tube

1. Introduction

Concrete filled steel tube columns (CFSTCs) possess numerous advantages over the conventional reinforced concrete and steel columns in both terms of structural performance and construction sequence, such as high compressive strength and fire resistance, large stiffness and ductility (Johansson and Gylltoft 2002). Moreover, the use of steel tube as a permanent formwork and thus reduces the construction cost and the amount of labor (Han *et al*. 2014). Consequently, in recent decades, the pace of CFSTCs has been increasing rapidly and their applications are more popular in multi-storey buildings, bridge piers and other supporting structures (Liew and Xiong 2012).

In practice, depending on type and function of CFSTCs in construction, load can be imposed on the concrete core or on the entire section. It is well known that when concentric load is applied only to the concrete core, the confinement induced by the steel tube is more efficient in comparison with the case where the steel tube and the concrete core are loaded simultaneously. According to Han *et al*. (2005) and Yu *et al*. (2010), for CFSTCs, it is recommended that only the concrete core is to be loaded in order to obtain better strength and ductility, which are amongst the most important design factors. This loading pattern refers to the form of the steel tube confined concrete (STCC) columns as shown in Fig. 1.

Within the last two decades, the use of ultra high performance concrete (UHPC) has been gaining increasing popularity in the civil engineering community owing to the superior performance and continued advancement of material technology (Schmidt and Fehling 2005). UHPC with compressive strength up to 200 MPa exhibits enormous compressive brittleness and steel fiber plays little act in improving compressive ductility, so it is necessary to utilize steel tubes to alleviate the brittleness of UHPC (Yan and Feng 2008, Fehling *et al*. 2014). With regard to the concrete compressive strength classification, ultra high strength concrete (UHSC) is usually defined as concrete with cylinder compressive strength exceeding 120 MPa (Liew and Xiong 2015), while UHPC refers to the

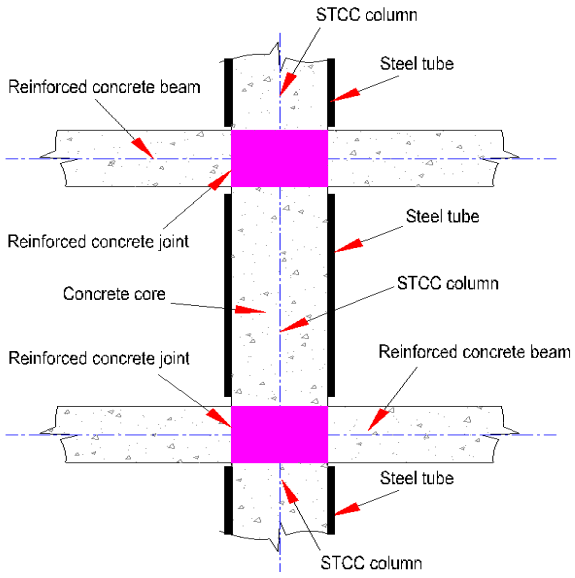

Fig. 1 A schematic view of the STCC columns (following Yu *et al*. 2010)

*Corresponding author, Ph.D. Student,
E-mail: lehoangancdv@gmail.com
[a] Professor, E-mail: fehling@uni-kassel.de

ISSN: 1229-9367 (Print), 1598-6233 (Online)

cylindrical concrete specimens with the compressive strengths greater than 150 MPa (Fehling *et al*. 2014). Both UHSC and UHPC exhibit very high strength and secant modulus compared to normal strength concrete (NSC) and high strength concrete (HSC), however it should be noted that UHSC and UHPC are not synonymous (Liew and Xiong 2015). In addition to the higher packing density of fines and compressive strength, which is defined for UHSC, the term "Ultra High Performance" refers to the outstanding durability and low ratio water/cement (Fehling *et al*. 2014).

UHPC or UHSC filled steel tube columns (UHPC-FSTCs or UHSC-FSTCs) can exploit the best attributes of both steel tube and concrete core, thus allowing engineers to reduce the cross section, to economize on concrete and to achieve small dead load owing to very high compressive strength while still obtaining increased stiffness, strength, energy absorption and ductility. As a consequence, UHPC is an attractive alternative to NSC and HSC for CFSTCs (Liew and Xiong 2012). It has been found that although there have been many studies on NSC filled in steel tube columns (NSC-FSTCs) or HSC filled steel tube columns (HSC-FSTCs), there is relatively little research on UHPC-FSTCs or UHSC-FSTCs. On the other hand, current design codes for composite columns may be only applicable for NSC. For instance, Eurocode 4 (EC4 2004) limits the concrete strength class only up to C50/60, while American Institute of Steel Construction (AISC 2010) only applies to CFSTCs with normal weight concrete of compressive strengths between 21 MPa to 70 MPa, and the maximum concrete strength adopted in Architectural Institute of Japan (AIJ 2001) is 90 MPa. Hence, so as to accelerate the application of UHPC in CFSTCs and in order to extend the current design guidelines, further researches on UHPC-FSTCs are necessary.

It is well established that due to the smaller lateral deformation when using concrete with higher compressive strength, the confinement in CFSTCs employing HSC, UHSC and UHPC is less effective compared to that in NSC-FSTCs (Tue *et al*. 2004a, Yan and Feng 2008, Xiong 2012). More recently, several experimental studies have been conducted to examine the performance of circular UHPC-FSTCs or UHSC-FSTCs, such as Tue *et al*. (2004a, b), Schneider (2006), Yan and Feng (2008), Liew and Xiong (2010, 2012), Xiong (2012), Liew *et al*. (2014), Guler *et al*. (2013), Chu (2014), but more attentions have been paid to these columns subjected to the concentric loading on the entire section rather than on the concrete core. Based on the experimental findings, it is concluded that although UHPC-FSTCs can achieve very high load bearing capacities compared to NSC-FSTCs and HSC-FSTCs, the post-peak behavior is still brittle with the sudden failure after reaching the peak load which is induced by the natural brittleness of UHPC (Liew and Xiong 2010). Furthermore, it is also recommended that the confinement effect should be neglected in short circular UHPC-FSTCs under loading on the entire section (Yan and Feng 2008, Guler *et al*. 2013, Liew *et al*. 2014). It should be noted that, for CFSTCs, a short column is defined as length to diameter ratio smaller than 5 ($L/D \leq 5$) and this ratio usually varies from 2 to 5 (Tao *et al*. 2013). However, the columns loaded only on the concrete core possess sufficient performance on ductility and higher ultimate strength compared to those loaded on the entire section (Tue *et al*. 2004b, Liew and Xiong 2012, Xiong 2012). This may imply that research attention should be given to circular STCC columns using UHPC.

From the issues highlighted above, this study is conducted in the following steps: the previous experimental tests on circular STCC columns using various concrete strength are shortly summarized and overviewed; based on the test results of circular STCC stub columns using UHPC with cylinder compressive strengths higher than 150 MPa reported by Schneider (2006) and Xiong (2012), the influence of some key parameters such as the confinement factor, the ratio of diameter-to-steel thickness on the strength and the ductility are analysed and discussed in detail; the applicability of the current design codes (EC4, AISC and AIJ) and seven analytical models for confined concrete in circular CFSTCs are evaluated by the comparison of ultimate loads between predictions and test results. Finally, a simplified model is proposed to determine the stress-strain curves for confined UHPC in circular STCC stub columns and also verified by the comparison with the experimental stress-strain curves.

2. Overview of past experimental studies on STCC columns

After the early investigation presented by the research group led by Tomii (Tomii *et al*. 1985), several other experiments have been carried out in order to gain clear insights into the behavior of STCC columns, such as Sakino *et al*. (1985), Orito *et al*. (1987), O'Shea and Bridge (1997a, b), Johansson (2002), Johansson and Gylltoft (2002), Fam *et al*. (2004), Han *et al*. (2005), De Oliveira *et al*. (2010), Yu *et al*. (2010). Nevertheless, most of these studies have mainly concerned with circular cross section columns due to the significant increase in both strength and ductility as compared to rectangular and square ones (Schneider 1998). Studies have also shown that the axial strengths of the unbonded stub columns were slightly higher than those of the bonded ones, while the stiffness of the unbonded specimens was slightly reduced (Fam *et al*. 2004). The bonded columns are found to be more practical than the unbonded one, this is due to some complicated techniques are needed to create the unbonded interface between concrete and steel tube. Published research related to the performance of STCC columns included short columns (defined as length-to-diameter ratio $L/D \leq 5$) and slender columns ($L/D > 5$) (Tao *et al*. 2013).

An experimental program to examine the behavior of short circular thin-walled steel tubes (L/D of 3.5) filled with medium, high and very high strength concrete of 50, 80 and 120 MPa, respectively, and the diameter to steel thickness ratios varied between 60 and 220 was reported by O'Shea and Bridge (1997a, b, 2000). Some specimens were tested under loading on the concrete core in order to compare with the case of concentric and eccentric loading on the entire section. The authors mentioned that in all cases of loading patterns, the increase in steel tube thickness or eccentricity

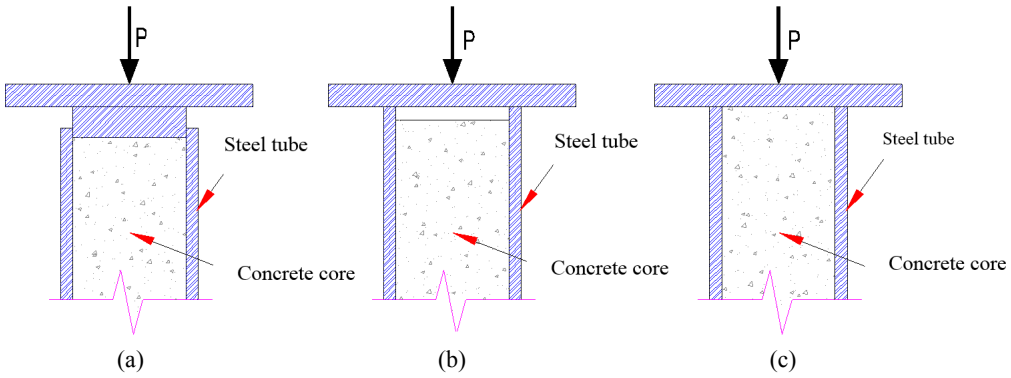

Fig. 2 Three types of loading application (following Johansson and Gylltoft 2002)

of loading leads to the improvement of the ductility. For the columns with high and very high strength concrete, the thicker tubes under concentric axial loading and at small applied eccentricities result in improved strength and ductility.

Johansson and Gylltoft (2002) presented the tests on short circular CFSTCs using the concrete core with the cylinder compressive strength of 64.5 MPa, the column length of 650 mm and the outer diameter of 159 mm under three types of load application as described in Fig. 2: load applied to (a) the concrete section, (b) the steel section and (c) the entire section. They stated that when the load is applied to the concrete core, a restraining effect of the steel tube on the concrete core appears as soon as the lateral deformation of the concrete core develops and thus the steel tube carries the longitudinal compression due to the activation of the bond at the steel-concrete interface. For this loading pattern, the bond strength and the confinement effect are closely related to each other. Furthermore, the confinement effect is found to be most pronounced in STCC stub columns compared to that in short CFSTCs loaded on the entire section or only on the steel tube. A similar observation was drawn in numerous studies such as Tomii *et al*. (1985), Orito *et al*. (1987), O'Shea and Bridge (1997a, b, 2000), Schneider (1998).

The behavior of slender circular STCC columns (L/D of 15.7) was also studied by Johansson and Gylltoft (2001). These authors pointed out that there is almost no difference in the axial load-deflection relationship when the load is applied to the entire section or only to the concrete core. For slender circular STCC columns, the changed bond strength has a significant influence on structural behavior as well as the force transferring from the concrete core to the steel tube. These authors also reached a conclusion that the beneficial effects of the composite behaviors on the confinement effect is not much for slender columns with the slenderness ratio of approximately 0.86 in their tests. This is in agreement with design code EC4 when the confinement effect is considered with the slenderness ratio less than 0.5.

The efficiency of passive confinement in short circular CFSTCs was investigated by Johansson (2002). The test variables in this study consisted of 12 columns using two concrete grades of C30 and C85, three different thicknesses of 5.0, 6.8 and 10 mm and two means of loading application: on the entire section and on the concrete core. The test results showed that only the values of the yielding load, the maximum load and the vertical deformation in the case of circular STCC stub columns were higher than those of CFSTCs loaded on the entire section, while the shapes of the axial load-deformation curves were not changed. Moreover, a suggestion was given that a thicker steel tube is necessary for the use of HSC in CFSTCs compared with NSC-FSTCs to obtain good ductility at the same level.

To evaluate the passive confinement provided by the steel tube in circular CFSTCs, De Oliveira *et al*. (2009, 2010) conducted a series of tests on circular STCC columns with various concrete strengths of 30, 60, 80 and 100 MPa. The other variables included four types of L/D ratios of 3, 5, 7 and 10 and two types of steel tube thicknesses of 3.35 mm and 6.0 mm. It was observed that all STCC columns with NSC core (30 MPa and 60 MPa) exhibited good ductility without loss of capacity after reaching the peak load. Nevertheless, for the STCC columns employing HSC (80 MPa and 100 MPa), the thicker tube resulted in better confinement effect of the concrete core.

An extensive experimental study on short and slender circular STCC columns under both monotonic and cyclic loading was reported by Han *et al*. (2005). It was pointed out that the sectional capacity of STCC stub columns is slightly higher than those of short CFSTCs loaded on the entire section, but the member capacity of STCC slender columns is slightly lower compared to that of slender CFSTCs loaded on the entire section. Furthermore, STCC columns are characterized by very high levels of energy dissipations and ductility. The authors noted that the prediction of ultimate strength for circular STCC columns from both design codes AIJ and AISC was conservative, while EC4 gave a slightly higher prediction.

As stated above, the published studies on circular STCC columns have focused mainly on NSC or HSC with the cylinder compressive strengths less than 120 MPa. More recently, research effort has been directed toward the application of UHPC and UHSC in STCC columns, where the cylinder compressive strengths of concrete are greater than 150 MPa. In the comprehensive research on CFSTCs using high strength materials conducted by Liew and Xiong (2010, 2012), Xiong (2012) and Liew *et al*. (2014), UHSC with compressive strengths varied between 150 MPa and 200 MPa and high strength steel tube with yield strength up to 700 MPa were employed. The behavior of short circular

UHSC-FSTCs was also examined under axial loading on the entire section and on the concrete core. It should be mentioned that UHSC mixture in this study was a commercial pre-blended mix mortar material. Steel fibers were added into the UHSC mixture in some specimens to investigate their influence on improving the ductility and the strength of composite columns. These authors recommended that the ductility and the strength of circular UHSC-FSTCs can be further improved by imposing the load only on the concrete core where the confinement effect becomes to be maximum. This recommendation implies that instead of circular CFSTCs loaded on the entire section, circular STCC columns should be considered if UHSC or UHPC is used.

A significant research effort to understand the behavior of UHPC-FSTCs was undertaken as a part of study on UHPC Hybrid Structures and reported by Tue *et al*. (2004a) and Schneider (2006). The extensive tests on short circular UHPC-FSTCs were conducted with various steel tube thicknesses ranged from 2.5 mm to 8.0 mm and the compressive strengths of UHPC cylinder greater than 150 MPa under loading on the concrete core and the entire section. In their study, UHPC mixture with coarse aggregate (Basalt split) and without steel fibers was used. Further tests on circular STCC stub columns using NSC and HSC with cylinder compressive strength of 36 MPa and 96 MPa, respectively, were also carried out to provide a deeper insight into the difference among short circular STCC columns using various concrete strengths (as shown in Fig. 3). The tests illustrated that circular STCC columns using NSC exhibited a remarkable ductile deformation capacity, while a small plastic deformation was found for the specimens using UHPC. The load versus strain relationship of short circular STCC columns using UHPC was observed to be quite similar to that of the specimens using HSC, however, the failure process was found to be more brittle with a steeper drop of load after attaining the peak load. The authors recommended that UHPC could be applicable for filling in STCC columns due to its higher stiffness and the reduction of required areas for steel and concrete, while the ultimate load and the deformation behavior remain the same compared to the use of HSC. However, these authors pointed out that UHPC has a strong autogenous shrinkage of approximately 0.5‰ which is much higher than NSC and HSC, thus leading to possible existence of a gap between

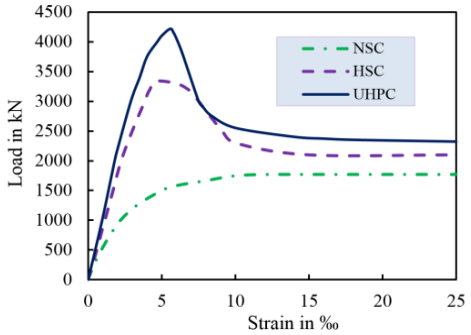

Fig. 3 Load versus vertical strain relationship for short circular STCC columns using NSC, HSC and UHPC (following Schneider 2006)

UHPC core and steel tube and a decrease in bond strength in steel-concrete interface. This phenomenon was confirmed by the fact that the values of strain gauges attached to the outer surface of steel tube in all the tests of STCC columns using UHPC were nearly zero until reaching about 50% of uniaxial cylinder strength (Tue *et al*. 2004a). On the other hand, for STCC columns, as stated by numerous studies (e.g., Johansson 2002, Fam *et al*. 2004), the confinement effect on the concrete core is greatly affected by the bond strength, this implies that the confinement effect might be less effective when UHPC is confined by steel tube.

With the current trend towards the use of UHPC-FSTCs in buildings and bridges, Tue *et al*. (2004b) proposed some application possibilities through an experimental investigation of UHPC-FSTCs for the joints in tall building and truss bridges with the use of concrete compressive strengths ranged between 150 and 180 MPa. It was highlighted that the abrupt load drop due to the inherent brittleness of UHPC core can be overcome by the sufficient confinement of the steel tube under predominant compression load such as loading on only the concrete core. This point of view was also generally supported by the advantages of circular STCC columns compared to conventional CFSTCs loaded on the entire section as described in previous research.

In summary, published studies on STCC columns, in general, and on UHPC-FSTCs, in particular, remain very limited with only a handful of experimental studies as mentioned above. Hence, this overview was aimed at contributing to a better understanding of the compressive behavior of circular STCC columns with the utilization of various concrete strengths. For practical application of UHPC in composite columns, further research on circular STCC columns using UHPC should be carried out. To date, apart from the tests presented by Tue *et al*. (2004a, b), Schneider (2006), Liew and Xiong (2010, 2012, 2014), Xiong (2012), no available research has been published on STCC columns using concrete with cylinder compressive strengths higher than 150 MPa. In addition to the limitation of experimental and theoretical works, the standard codes do not give any recommendations when UHPC or UHSC is used in STCC columns. This lack was the main motivation for this study.

3. Analysis of circular STCC stub columns using UHPC and discussion

A confinement factor ξ defined by many researchers such as Johansson (2002) and Yu *et al*. (2010) is used for circular STCC columns in this paper, i.e.

$$\xi = \frac{A_s . f_y}{A_c . f_c} \tag{1}$$

where A_s is the cross-sectional area of steel tube, A_c is the cross-sectional area of concrete core, f_y is the yield strength of steel tube, and f_c is the compressive strength of concrete cylinder.

For the convenience of comparisons between the ultimate loads of STCC columns and those of CFSTCs

Table 1 The main geometric and material characteristics of circular STCC stub columns using UHPC in the tests reported by Schneider (2006) and Xiong (2012)

Author	Specimen	$D \times t$ (mm)	L (mm)	f_c (MPa)	f_y (MPa)	N_{usSTCC} (kN)	$N_{usCFSTLES}$ (kN)	SI (%)
Schneider (2006)	NB2.5	164.2×2.5	652	166.8	377	3501	3490	0.32
	NB3.0	189.0×3.0	756	166.8	398	4837	4750	1.83
	NB4.0	168.6×3.9	648	174.2	363	4216	3920	7.55
	NB4.8	169.0×4.8	645	176.7	399	4330	4020	7.71
	NB5.0	168.7×5.2	645	170.5	405	4751	--	--
	NB5.6	168.8×5.7	650	173.4	452	4930	4450	10.79
	NB8.0	168.1×8.1	645	174.9	409	5254	--	--
Xiong (2012)	S1-2-1(a)*	114.3×6.3	210	173.5	428	2866	2309	24.12

loaded on the entire section, a strength index SI was also defined by Han *et al*. (2005) as follows

$$SI = \frac{N_{ueSTCC} - N_{ueCFSTLES}}{N_{ueCFSTLES}} \quad (2)$$

where N_{ueSTCC} and $N_{ueCFSTLES}$ are the ultimate loads of STCC columns and CFSTCs loaded on the entire section, respectively.

For the analysis in this section, the main geometric and material characteristics of circular STCC stub columns using UHPC obtained from Schneider (2006) and (Xiong 2012) were given in Table 1. It is well understood that there are many variables that affect to the strength as well as the ductility in circular STCC stub columns, such as the concrete compressive strength (f_c), length-to-diameter ratio (L/D), diameter-to-thickness ratio (D/t), the confinement factor ξ and the yield stress of steel tube (f_y). Nevertheless, there is very limited analytical work on the influence of these variables to the performance of circular STCC columns using UHPC. Thus, in this paper, the influence of D/t ratio and the confinement factor ξ on the ultimate strength and the ductility were discussed.

3.1 Comparison between circular STCC columns using UHPC and circular UHPC-FSTCs loaded on entire section

In the test program conducted by Schneider (2006) and Xiong (2012), circular UHPCFST stub columns with steel tube thicknesses of 2.5, 3.0, 3.9, 4.8, 5.7 mm and 6.3 mm, respectively, were loaded in both cases: on the concrete core and the entire section. Based on these test results, the strength index SI was calculated and listed in Table 1. Overall, with the same geometric and material parameters, the ultimate compressive strengths of circular STCC columns using UHPC are higher than circular UHPC-FSTCs loaded on the entire section. For the specimens in Schneider (2006), the values of SI ranged from 0.32 to 10.95 when the steel tube thicknesses changed from 2.5 mm to 5.7 mm. It is also found in Table 1 that SI increased up to 24.12 for the specimen of Xiong (2012).

Han *et al*. (2005) asserted that there are some discrepancies between the features of STCC columns and CFSTCs loaded on the entire section. To clarify this point of view, load versus strain curves of circular STCC columns and CFSTCs loaded on entire section using UHPC with cylinder compressive strength of 174.2 MPa, steel tube thickness of 4.0 mm, outer diameter of 168.6 mm were plotted in Fig. 4. For both loading patterns, the increase of load path is mostly linear before the first peak load, followed by an abrupt load drop and then a horizontal plateau occurs after the second peak load. More importantly, the ultimate strength and the ultimate strain of STCC column are larger than those of CFSTCs loaded on the entire section. This is due to the fact that the confinement effect in circular STCC columns is more efficient in comparison with circular CFSTCs loaded on entire section where the confinement effect is small and both the steel tube and the concrete core act separately until failure (Tue *et al*. 2004a).

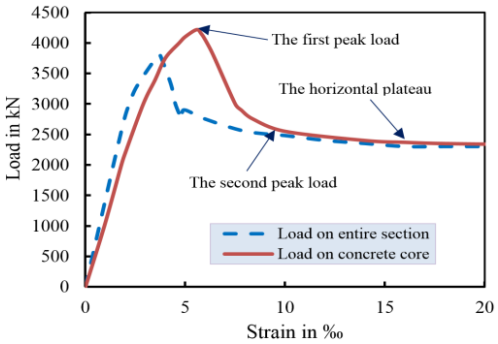

Fig. 4 Load versus strain curve of circular STCC columns and UHPC-FSTCs under loading on the entire section (following Schneider 2006)

It has been suggested that the confinement effect in short circular UHPC-FSTCs under loading on the entire section should be neglected in the calculation of ultimate strength (Guler *et al*. 2013, Liew *et al*. 2014). However, from the observations as mentioned above, the circular STCC stub columns using UHPC are found to exhibit a better confinement effect by which both the strength and the ductility are well improved. Hence, in contradistinction to circular UHPC-FSTCs under loading on the entire section, the confinement effect exerted by the steel tube must be considered for determining the strength and the ductility in circular STCC stub columns using UHPC.

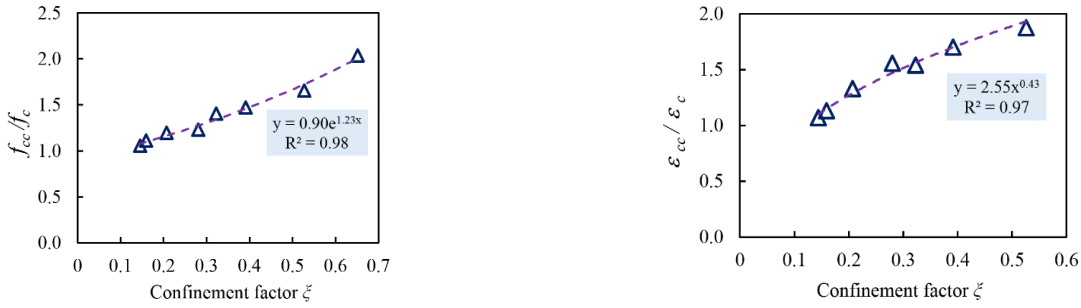

(a) (b)

Fig. 5 (a) The ratio f_{cc}/f_c versus the confinement factor ξ; and (b) the ratio $\varepsilon_{cc}/\varepsilon_c$ versus the confinement factor ξ

3.2 The influence of the confinement factor ξ

For convenience of comparison and analysis in this study, the confined peak strength f_{cc} and the residual strength f_r was used. The values of f_{cc} and f_r are calculated using the ratio of ultimate load (N_{ueSTCC}) and the second peak load (N_r) to concrete cross-sectional area (A_c), respectively

$$f_{cc} = \frac{N_{ueSTCC}}{A_c} \tag{3}$$

$$f_r = \frac{N_r}{A_c} \tag{4}$$

It should be mentioned that N_r is the second peak load where the axial load – strain curve is supposed to be approximately horizontal (see Fig. 4).

It is also important to find that the strain of UHPC core in Schneider's tests was directly measured over a length of 300 mm using three Linear Varying Displacement Transducers (LVDTs) which monitored the displacement of steel bars positioned in the concrete core through an arrangement of drillings in the steel tube (see Tue *et al.* 2004a, Schneider 2006). Therefore, the confined strain ε_{cc} corresponding to the confined peak strength f_{cc} can be taken from the results of measurement in Schneider (2006).

Figs. 5(a)-(b) show the relations between the ratio f_{cc}/f_c, $\varepsilon_{cc}/\varepsilon_c$ and the confinement factor ξ. The ratios f_{cc}/f_c and $\varepsilon_{cc}/\varepsilon_c$ are found to be increased with increasing the confinement factor ξ. This is attributed to the fact that higher confinement factor ξ can trigger better constraining effect between the steel tube and the concrete core by which the strength and the strain are better enhanced. When the confinement factor ξ increases to more than 0.5, the ratios f_{cc}/f_c and $\varepsilon_{cc}/\varepsilon_c$ are larger than 1.5. The relation between the ratio f_r/f_{cc} and the confinement factor ξ is plotted in Fig. 6. It can be seen that the increase in the confinement factor ξ results in higher value of the ratio f_r/f_{cc}. When the confinement factor ξ is higher than 0.3, the ratio f_r/f_{cc} is larger than 0.7. It is suggested by Liew *et al.* (2014) that to ensure a safe design for CFSTCs, the residual resistance should be at least equal to 70% of the designed ultimate resistance, which means that the ratio f_r/f_{cc} should not be lower than 0.7. Therefore, it can be recommended that, for circular STCC stub columns using UHPC, the confinement factor ξ should be greater than 0.3 to satisfy this suggestion.

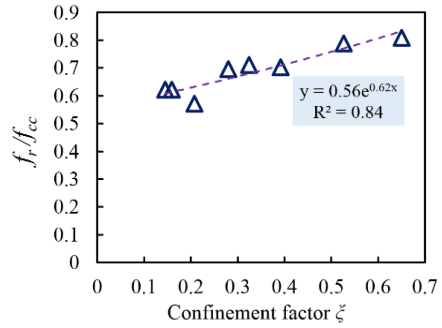

Fig. 6 The ratio f_{cc}/f_c versus the confinement factor ξ

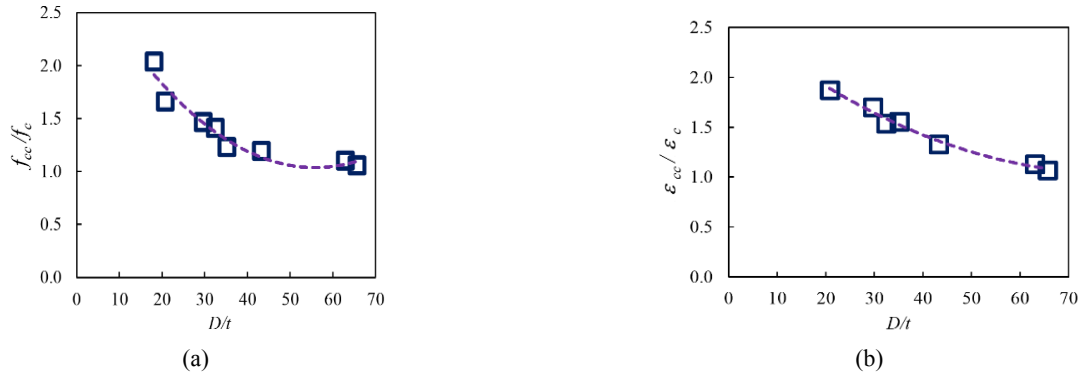

(a) (b)

Fig. 7 (a) The ratio f_{cc}/f_c versus the ratio D/t; and (b) the ratio of $\varepsilon_{cc}/\varepsilon_c$ versus the ratio D/t

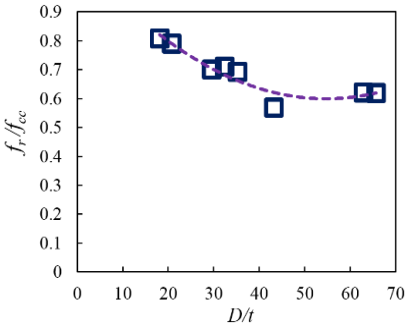

Fig. 8 The ratio f_r/f_c versus the ratio D/t

Table 2 Range of applicability of design codes

Code	f_c (MPa)	f_y (MPa)	Steel thickness t (mm)
EC4 (2004)	$20 \le f_c \le 60$	$235 \le f_y \le 460$	$t \ge \frac{D.f_y}{90 \cdot 235(MPa)}$
AISC (2010)	$21 \le f_c \le 70$	$f_y \le 525$	$t \ge \frac{D \cdot f_y}{0.15 \cdot E_s}$
AIJ (2001)	$18 \le f_c \le 90$	$235 \le f_y \le 440$	$t \ge \frac{D \cdot f_y}{35250}$

3.3 The influence of diameter-to-thickness ratio (D/t)

It is evident from the relation between the ratio f_{cc}/f_c and the ratio D/t, as well as the relation between the ratio $\varepsilon_{cc}/\varepsilon_c$ and the ratio D/t plotted in Figs. 7(a)-(b) that smaller ratio of D/t leads to higher ratio of f_{cc}/f_c and $\varepsilon_{cc}/\varepsilon_c$. The ratios f_{cc}/f_c and $\varepsilon_{cc}/\varepsilon_c$ are significantly increased by between 1.5 and 2.0 when the ratio D/t is lower than 30, whereas for D/t ratio greater than 60, the ratio f_{cc}/f_c and $\varepsilon_{cc}/\varepsilon_c$ are approximately equal to 1.0. Therefore, it is indicated that for circular STCC stub columns using UHPC, the value of D/t ratio should be lower than 30 to obtain more pronounced confinement effect provided by the steel tube, this may effectively enhance the ultimate compressive strength and strain of the columns.

In terms of the ratio f_r/f_{cc}, it can be found from the Fig. 8 that there is also an increase of f_r/f_{cc} ratio when using smaller D/t ratio. When D/t ratio is lower than 30, the ratio of f_r/f_{cc} is greater than 0.7. Therefore, the value of D/t ratio should be smaller than 30 to achieve a reasonable ductility following the suggestion made by Liew *et al*. (2014).

3.4 Comparison of test results with EC4, AISC and AIJ

Provisions from three different building codes (EC4, AISC and AIJ) were used to calculate the ultimate loads of 8 specimens in Table 1 and then compared with the test results. It is noted that the material partial safety factors in the codes were set to unity in this study.

Table 3 presents the comparison of ultimate loads between code predictions (N_{pre}) and experimental results (N_{ue}). It is worth noting that circular STCC stub columns using UHPC were out of the range of application of the code formulations as shown in Table 2 because the compressive strengths of UHPC cylinder exceed 150 MPa.

The results of comparison presented in Table 3 indicated that both AISC and AIJ are conservative for predicting the ultimate loads of circular STCC columns using UHPC. More precisely, AISC gave a ultimate load about 14.2% lower than the test results, while AIJ gave a ultimate load approximately 7.5% lower than those of the measured results. Thus, the predictions of ultimate loads from both AISC and AIJ were on the safe side. However, on average, EC4 overestimated the ultimate load by about 4.5% higher than those from experimental results, and gave an unsafe prediction. Furthermore, EC4 gave better predicted ultimate loads for the columns with thicker steel tube walls than those with thinner walls, but for the specimens with thinner steel tube walls, AISC and AIJ can be used since they provide reliable predictions compared to the test results.

Overall, both AIJ code and EC4 code were able to estimate the ultimate loads with small difference compared to the test results. Among three codes, it can be concluded that AIJ with a mean value of 0.925 and a COV of 0.055 is the best and the safest predictor to calculate the ultimate loads of circular STCC short columns employing UHPC.

Table 3 Comparisons of ultimate loads between design codes and test results in Table 1

Author	Specimen	N_{ue} (kN)	EC4 (2004)		AISC (2010)		AIJ (2001)	
			N_{pre} (kN)	$\frac{N_{pre}}{N_{ue}}$	N_{pre} (kN)	$\frac{N_{pre}}{N_{ue}}$	N_{pre} (kN)	$\frac{N_{pre}}{N_{ue}}$
Schneider 2006	NB2.5	3501	3987.07	1.139	3136.58	0.896	3428.54	0.979
	NB3.0	4837	5343.97	1.105	4204.00	0.869	4612.86	0.954
	NB4.0	4216	4514.35	1.071	3695.79	0.877	3935.26	0.933
	NB4.8	4330	4792.18	1.107	3980.00	0.919	4249.79	0.981
	NB5.0	4751	4721.49	1.001	3944.65	0.837	4223.98	0.896
	NB5.6	4930	4977.72	1.010	4183.75	0.849	4542.19	0.921
	NB8.0	5254	5139.95	0.978	4414.52	0.840	4806.53	0.915
Xiong 2012	S1-2-1(a)*	2866	2717.38	0.948	2226.55	0.777	2358.67	0.823
Mean value				1.045		0.858		0.925
COV (Coefficient of Variation)				0.067		0.050		0.055

Table 4 Expressions for calculating the predicted ultimate loads by using seven analytical models

Model	Expressions	Explanations
Susantha *et al*. (2001)	$v_c' = \frac{0.881}{10^6}\cdot\left(\frac{D}{t}\right)^3 - \frac{2.58}{10^4}\cdot\left(\frac{D}{t}\right)^2 + \frac{1.953}{10^2}\left(\frac{D}{t}\right) + 0.4011$ $v_c = 0.2312 + 0.3528\cdot v_c' - 0.1524\cdot\left(\frac{f_c}{f_y}\right) + 4.843\cdot v_c'\left(\frac{f_c}{f_y}\right) - 9.169\cdot\left(\frac{f_c}{f_y}\right)^2 \quad \beta = v_c - v_s$ and $f_{rp} = \beta\cdot\frac{2\cdot t}{D-2\cdot t}\cdot f_y$ $f_{cc} = f_c + 4\cdot f_{rp}$ and $N_u = A_c\cdot f_{cc} + A_s\cdot fy$	v_c and v_s: Poisson ratio of a steel tube filled with concrete and a steel in yield condition f_{rp}: Lateral pressure at the peak load f_{cc}: Confined compressive strength of the concrete N_u: Axial capacity of CFST column
Hatzigeorgiou (2008)	$\sigma_h = f_y\cdot\exp\left[\ln\left(\frac{D}{t}\right) + \ln(f_y) - 11\right]$ $f_{rp} = \frac{2\cdot t}{D-2\cdot t}\cdot\sigma_h$ and $f_{cc} = f_c + 4.3\cdot f_{rp}$ $f_{yc} = 0.5\cdot\left(\sigma_h - \sqrt{4\cdot f_y^2 - 3\cdot\sigma_h^2}\right); \quad N_u = A_c\cdot f_{cc} + A_s\cdot f_{yc}$	σ_h: Hoop stress of the steel f_{rp}: Mean confining stress f_{yc}: Compressive yield stress of steel tube
Johansson (2002)	$v_a = 0.3, v_c = 0.2, \varepsilon_v = 0.002$ $\varepsilon_{ahr} = \frac{\varepsilon_v(v_a - v_c)}{\left[1 + \frac{2\cdot t\cdot E_a}{(D-2\cdot t)\cdot E_c}\right]}$ and $\varepsilon_{ah} = -v_a\cdot\varepsilon_v + \varepsilon_{ahr}$ $\sigma_{ah} = \frac{E_a}{1-v_a^2}\cdot(\varepsilon_{ah} + v_a\cdot\varepsilon_{al}); \quad \sigma_{al} = \frac{E_a}{1-v_a^2}\cdot(\varepsilon_v + v_a\cdot\varepsilon_{ah})$ $\sigma_{lat} = \sigma_{ah}\cdot\frac{2\cdot t}{D-2\cdot t}$ and $k = 1.25\cdot\left(1 + 0.062\cdot\frac{\sigma_{lat}}{f_{ct}}\right)\cdot f_c^{-0.21}$ $f_{cc} = f_c\cdot\left(\frac{\sigma_{lat}}{f_{ct}} + 1\right)^k$ and $N_u = A_c\cdot f_{cc} + A_s\cdot\sigma_{al}$	v_a, v_c, ε_v: Initial considered values ε_{ahr}: Restrained steel strain ε_{ah}: Final lateral strain of steel σ_{ah}: Steel's lateral stress σ_{al}: Steel's longitudinal stress σ_{lat}: Compressive confining pressure k: Parameter that reflects the effectiveness of confinement f_{ct}: Tensile strength of concrete
Sakino *et al*. (2004)	$\sigma_{ccB} = \gamma_u\cdot f_c + 4.1\cdot\sigma_r; \quad \gamma_u = 1.67\cdot D_c^{-0.112}$ $\sigma_r = \frac{-2\cdot t}{D-2\cdot t}\cdot\sigma_{s\theta}; \quad \sigma_{s\theta} = \alpha_u\cdot\sigma_{sy}$ and $\sigma_{sz} = \beta_{uc}\cdot\sigma_{sy}, \quad \alpha_u = -0.19; \beta_{uc} = 0.89$ $N_u = A_c\cdot\sigma_{ccB} + A_s\cdot\sigma_{sz}$	σ_{ccB}: Strength of confined concrete γ_u: Strength reduction factor for concrete σ_r: Lateral pressure $\sigma_{s\theta}$: Hoop stress of steel tube in yield condition and σ_{sy}: Tensile yield stress of steel σ_{sz}: Axial yield stress of steel tube
Liang and Fragomeni (2009)	$f_{cc} = \gamma_c\cdot f_c + k_1\cdot f_{rp}$ $f_{rp} = \begin{cases} 0.7\cdot(v_e - v_s)\cdot\frac{2\cdot t}{D-2\cdot t}\cdot f_{sy} & (\frac{D}{t}\le 47) \\ \left(0.006241 - 0.0000357\cdot\frac{D}{t}\right)\cdot f_{sy} & (47 < \frac{D}{t}\le 150) \end{cases}$ $v_e = 0.2312 + 0.3528\cdot v_e' - 0.1524\cdot\left(\frac{f_c}{f_{sy}}\right) + 4.843\cdot v_c'\left(\frac{f_c}{f_{sy}}\right) - 9.169\cdot\left(\frac{f_c}{f_{sy}}\right)^2$ $v_e' = \frac{0.881}{10^6}\cdot\left(\frac{D}{t}\right)^3 - \frac{2.58}{10^4}\cdot\left(\frac{D}{t}\right)^2 + \frac{1.953}{10^2}\left(\frac{D}{t}\right) + 0.4011$ $\gamma_c = 1.85\cdot D_c^{-0.135}\left(0.85\le\gamma_c\le 1\right)$ $\gamma_s = 1.458\cdot\left(\frac{D}{t}\right)^{-0.1}\left(0.9\le\gamma_s\le 1.1\right)$ $N_u = \left(\gamma_c\cdot f_c + 4.1\cdot f_{rp}\right)\cdot A_c + \gamma_s\cdot f_{sy}\cdot A_s$	f_{cc}: Strength of confined concrete f_{rp}: Lateral pressure γ_c: Strength reduction factor for concrete γ_s: Strength factor for the steel tube f_{sy}: Tensile yield strength of steel v'_e: Empirical factor v_e: Poisson ratio of a steel tube filled with concrete

3.5 Comparison between test results and analytical models

It is commonly accepted that the confinement action exerted by the steel tube on the concrete core is of passive type and it increases the ultimate strength of the concrete core significantly. The confinement effect has been studied for many years, and the confinement level mainly depends

Table 4 Continued

Model	Expressions	Explanations
Zhong and Miao (1988)	$p_o = -\frac{\alpha}{2}\cdot\frac{2\cdot\mu'+1}{\left[3\cdot\left(\mu'^2+\mu'+1\right)\right]^{1/2}}\cdot f_y$ $\mu' = -\frac{1}{2}-\frac{1}{2\cdot(\zeta+1)}$ $\zeta = \alpha\cdot\frac{f_y}{f_c};\alpha=\frac{A_s}{A_c}$ $N_u = N_c + N_s$ $N_s = \frac{\mu'+2}{\left[3\cdot\left(\mu'^2+\mu'+1\right)\right]^{1/2}}\cdot f_y\cdot A_s$ $N_c = \left(f_c+4\cdot p_o\right)\cdot A_c$	p_o: Lateral confining pressure of the steel tube on the concrete N_c: Sectional strength of concrete core N_s: Sectional strength of steel tube
O'Shea and Bridge (2000)	$f_{cc} = f_c\cdot\left(-1.228+2.172\cdot\sqrt{1+\frac{7.46 f_l}{f_c}}-2\cdot\frac{p}{f_c}\right)\left(f_c\le 50\text{ MPa}\right)$ $\frac{f_{cc}}{f_c} = \left(\frac{p}{f_t}+1\right)^k \quad \left(80\text{ MPa}\le f_c\le 100\text{ MPa}\right)$ $p = p_{yield}\cdot\left(0.7-\sqrt{\frac{f_c}{f_y}}\right)\cdot\left(\frac{10}{3}\right)$ $p_{yield} = \frac{2\cdot f_y\cdot t}{D-2t}$ $k = 1.25\cdot\left(1+0.062\cdot\frac{p}{f_c}\right)\cdot\left(f_c\right)^{-0.21}$ $f_t = 0.558\sqrt{f_c}$ and $N_u = A_c\cdot f_{cc} + A_s.f_y$	f_{cc}: Compressive strength of confined concrete p: The applied confining pressure f_y: Yield strength of steel tube f_t: Tensile strength of concrete p_{yield}: The confining pressure in yield condition k: Parameter that reflects the effectiveness of confinement

on the lateral confining stress. It has been found that, to be realistic, the value of lateral confining stress must be correctly determined in order to calculate the ultimate strength of column under any given type of loading. However, the experimental measurement of lateral confining stress at any section of columns requires sophisticated equipment. As a consequence, to reduce the cost and the time for testing, various analytical models were proposed by different researchers for evaluating the ultimate strengths of CFSTCs with taking into account the passive confinement effect. Furthermore, in most of existing confining stress models, the formulae were built up by using the confining theory and experiments, but mainly related to CFSTCs using NSC or HSC. There are also discrepancies in both the lateral confining stress and the ultimate strength predicted by these models due to different approaches in the processes of establishing the formulae.

In the extensive study on the behavior of circular STCC columns with wide range of length to diameter ratios (L/D = 3, 5, 7 and 10) and various concrete compressive strengths (32.7, 58.7, 88.8 and 105.5 MPa) presented by De Oliveira *et al*. (2010), the passive confinement was evaluated using the comparison of the axial load capacities between the test results and three analytical models proposed by Johansson (2002), Susantha *et al*. (2001) and Hatzigeorgiou (2008). The authors pointed out that the three analytical models provided good prediction for the axial load capacity, but for slender columns with the ratio L/D higher than 3, a new factor was introduced to correct the values of predictions. Currently, apart from the study in De Oliveira *et al*. (2010), the research on the verification of the previous confining stress models for circular STCC columns using HSC, in general, and using UHPC, in particular, remain very limited. The suitability of existing confinement models for UHPC in circular STCC columns should be further considered. Therefore, in this paper, seven analytical models proposed by Susantha (Susantha *et al*. 2001), Hatzigeorgiou (2008), Johansson (2002), Sakino *et al*. (2004), Liang and Fragomeni (2009), Zhong and Miao (1988), O'Shea and Bridge (2000) were selected for calculating the ultimate loads of 8 specimens in Table 1 and then the suitability of these models was judged by the comparison with test results.

Table 4 shows the sequence of expressions in the seven analytical models to predict the ultimate loads of circular STCC stub columns. The comparison of the ultimate loads between the seven analytical models (N_{pre}) and the test results (N_{ue}) was illustrated in Table 5.

As seen from the mean values of the predicted ultimate load to experimental ultimate load ratios (N_{pre}/N_{ue}) in the Table 5, all models provided an estimation of the ultimate loads with excellent accuracy compared to those measured in the tests by Schneider (2006) and Xiong (2012). On average, the highest ratio N_{pre}/N_{ue} is 1.056 in Johansson's model, while the model of Zhong and Miao (1988) gave the smallest ratio N_{pre}/N_{ue} of 0.971.

Analyzing these mean values, the predicted ultimate loads in the models proposed by Susantha (Susantha *et al*.

Table 5 Comparisons of ultimate loads between analytical models and test results

Author	ID	N_{ue} (kN)	Susantha (2001)		Hatzigeorgiou (2008)		Johansson (2002)	
			N_{pre} (kN)	$\frac{N_{pre}}{N_{ue}}$	N_{pre} (kN)	$\frac{N_{pre}}{N_{ue}}$	N_{pre} (kN)	$\frac{N_{pre}}{N_{ue}}$
Schneider 2006	NB2.5	3501	3875.87	1.107	4085.34	1.167	4041.75	1.155
	NB.,0	4837	5122.18	1.059	5506.58	1.138	5371.83	1.111
	NB4.0	4216	4582.32	1.087	4555.70	1.081	4629.44	1.098
	NB4.8	4330	4738.34	1.094	4858.95	1.122	4886.77	1.129
	NB5.0	4751	4562.54	0.968	4790.70	1.016	4809.88	1.020
	NB5.6	4930	4791.14	0.972	5131.37	1.041	4950.19	1.004
	NB8.0	5254	5800.44	1.104	5183.38	0.987	5380.22	1.024
Xiong 2012	S1-2-1(a)*	2866	2791.86	0.974	2498.09	0.872	2612.50	0.912
Mean value			1.046		1.053		1.056	
COV (Coefficient of Variation)			0.061		0.091		0.076	

Author	ID	N_{ue} (kN)	Sakino *et al.* (2004)		Liang and Fragomeni (2009)		Zhong and Miao (1988)		O'Shea and Bridge (2000)	
			N_{pre} (kN)	$\frac{N_{pre}}{N_{ue}}$	N_{pre} (kN)	$\frac{N_{pre}}{N_{ue}}$	N_{pre} (kN)	$\frac{N_{pre}}{N_{ue}}$	N_{pre} (kN)	$\frac{N_{pre}}{N_{ue}}$
Schneider 2006	NB2.5	3501	3750.29	1.071	3657.38	1.050	3795.10	1.084	3770.00	1.077
	NB3.0	4837	4973.79	1.028	4858.31	1.004	5078.82	1.050	5181.12	1.071
	NB4.0	4216	4272.76	1.013	4248.05	1.008	4262.11	1.011	4119.99	0.977
	NB4.8	4330	4587.39	1.059	4458.87	1.030	4498.73	1.039	4620.90	1.067
	NB5.0	4751	4546.37	0.964	4411.00	0.936	4417.15	0.937	4729.44	1.003
	NB5.6	4930	4866.09	0.987	4601.25	0.933	1662.10	0.946	5378.91	1.091
	NB8.0	5254	5110.88	0.973	5452.54	1.038	4774.76	0.909	5727.89	1.004
Xiong 2012	S1-2-1(a)*	2866	2551.07	0.89	2473.80	0.863	2281.01	0.796	2679.26	0.935
Mean value			0.998		0.983		0.971		1.028	
COV (Coefficient of Variation)			0.058		0.066		0.097		0.055	

2001), Hatzigeorgiou (2008), Johansson (2002) and O'Shea and Bridge (2000) were slightly higher than those in the experimental tests with the average differences ranged from 2.8% to 5.6%, giving the unsafe side. It is also evident from the comparison in Table 5 that the predictions of the models of Sakino *et al*. (2004), Zhong and Miao (1988) and Liang and Fragomeni (2009) presented the average differences of 0.2%, 2.9% and 1.7% with corresponding COV of 0.058, 0.097 and 0.066, respectively as compared to the test results, being on the safe side. However, the values of COV in the models assumed by Hatzigeoriou (2008) and Zhong and Miao (1988) were higher than those of the other models with the values of 0.091 and 0.097, respectively, showing a large scatter in predictions

In general, seven models were able to accurately predict the ultimate loads of the columns tested by Schneider (2006) and Xiong (2012). Among these models, the models of Sakino *et al*. (2004) is the best predictor to calculate the ultimate load of circular STCC stub columns using UHPC due to the smallest difference (N_{pre}/N_{ue} = 0.998) and the safe predictions compared to the test results, as described above. Nevertheless, additional tests on circular STCC columns using UHPC are much needed to further verify the effectiveness of these models, and then the sequence of procedures to predict the lateral confining stress as well as the ultimate load in each model may be modified.

4. Simplified model for stress-strain curve of UHPC confined by steel tube columns

It is a well-known fact that, UHPC core in circular STCC short columns experiences an enhanced compressive strength and an apparent ductility because of the confinement effect from steel tube. However, it has been also shown that confined UHPC does not exhibit the same increase in concrete compressive strength and ductility as confined NSC and confined HSC (Tue *et al*. 2004a, Yan and

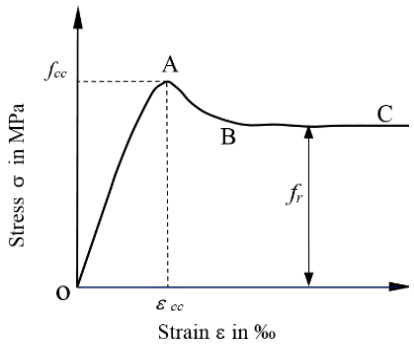

Fig. 9 Stress-strain model proposed for UHPC confined by circular steel tube stub columns

Feng 2008). For circular CFSTCs, although there are many stress-strain models of confined concrete assumed by various authors, these models may not be suitable for all concrete strength, particularly for UHPC because that UHPC as a new innovative cementitious material exhibits very different characteristics compared to NSC and HSC. Therefore, it is necessary to develop a model to propose a stress-strain curve for UHPC confined by steel tube stub columns with considering the confinement effect. This study presents a simplified model based on the test results by Schneider (2006) and Xiong (2012) and some modifications of the models proposed by Binici (2005), Tao *et al*. (2013) and Samani and Attard (2012).

To reflect the experimental evidence, a general stress-strain curve depicted in Fig. 9 is used to describe the compressive behavior of confined UHPC in circular STCC stub columns.

The ascending stress-strain (σ-ε) curve (OA) is represented using the equations suggested by Samani and Attard (2012) as follows

$$Y = \frac{A \cdot X + B \cdot X^2}{1 + (A-2) \cdot X + (B+1) \cdot X^2} \quad \text{when} \quad 0 \le \varepsilon \le \varepsilon_{cc} \tag{5}$$

where

$$Y = \frac{\sigma}{f_{cc}} \quad \forall \quad 0 \le Y \le 1 \tag{6}$$

$$X = \frac{\varepsilon}{\varepsilon_{cc}} \quad \forall \quad X \ge 0 \tag{7}$$

$$A = \frac{E_c \cdot \varepsilon_{cc}}{f_c} \tag{8}$$

$$B = \frac{(A-1)^2}{0.55} - 1 \tag{9}$$

It is found that the confined concrete strength f_{cc} and its corresponding strain ε_{cc} can be expressed as functions of confinement factor ξ. Hence, f_{cc} and ε_{cc} are computed by the following equations proposed by the regression analysis in Figs. 5(a)-(b)

$$\frac{f_{cc}}{f_c} = 0.9 \cdot e^{1.23 \cdot \xi} \tag{10}$$

$$\frac{\varepsilon_{cc}}{\varepsilon_c} = 2.55 \cdot \xi^{0.43} \tag{11}$$

where the strain ε_c at the peak stress of unconfined UHPC cylinder and the elastic modulus E_c are calculated according to the Eqs. (13)-(14). These equations were proposed by Schneider (2006) based on the regression analysis of test results for UHPC cylinders under uniaxial compression3

$$\varepsilon_c = 0.00083 \cdot f_c^{0.276} \tag{12}$$

$$E_c = 10200 \cdot f_c^{1/3} \tag{13}$$

For the descending branch of the confined concrete model (ABC), an exponential function proposed by Binici (2005) is used and given by

$$\sigma = f_r + (f_{cc} - f_r) \exp\left[-\left(\frac{\varepsilon - \varepsilon_{cc}}{\alpha} \right)^{\beta} \right] \quad \text{when} \quad \varepsilon > \varepsilon_{cc} \tag{14}$$

In which f_r is the residual stress as shown in Fig. 9. The expression for f_r can be proposed by the result of regression analysis in Fig. 6(a) as follows

$$\frac{f_r}{f_{cc}} = 0.56 \cdot e^{0.62 \cdot \xi} \tag{15}$$

where α and β are parameters determining the shape of the softening branch. The value of α is determined by the expression proposed by Tao *et al*. (2013) as follows

$$\alpha = 0.04 - \frac{0.036}{1 + e^{6.08 \cdot \xi - 3.49}} \tag{16}$$

To ensure the predicted softening branch of stress-strain (σ-ε) curves match with measured values closely, different trial values of β were adopted to obtain the best-fit values. It was found that when β was equal to 15, the predicted curves were acceptable compared with the experimental curves. Thus, in this study, β is taken as 15.

The actual stress-strain of confined UHPC of seven circular STCC stub columns with various steel tube thicknesses measured in the tests reported by Schneider (2006) were used to verify the proposed model. Figs. 10-13 performed the comparison of complete stress-strain curve of confined UHPC between the proposed model and the test results to verify the prediction accuracy. As evident from the comparisons, the predictions of the proposed model are in good agreement with the experimental results, which consist of a wide range of steel tube thickness ranging from 2.5 mm to 8.1 mm and cylinder concrete compressive strengths between 166.8 to 176.7 MPa. The proposed model gives reasonable ascending parts of the curves compared to experimental tests. Furthermore, the sudden load drop in the softening branch of stress-strain curve right after the first

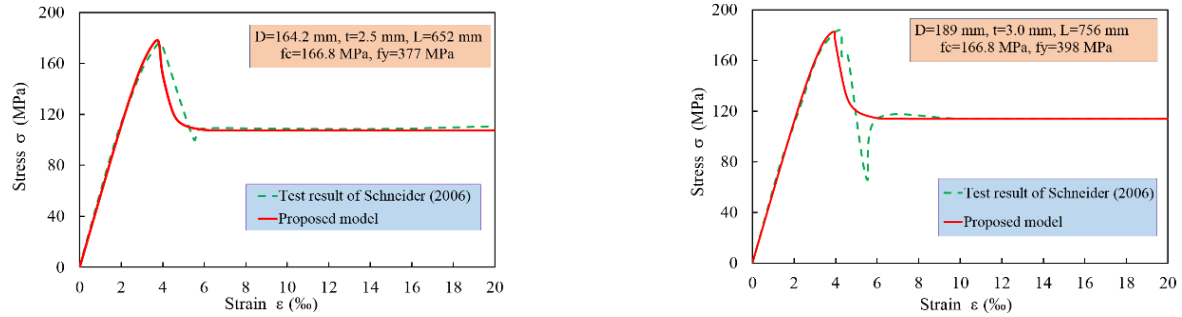

(a) (b)

Fig. 10 Comparison of stress-strain curves between proposed model and test results for columns with steel thicknesses (a) t = 2.5 mm; and (b) t = 3.0 mm

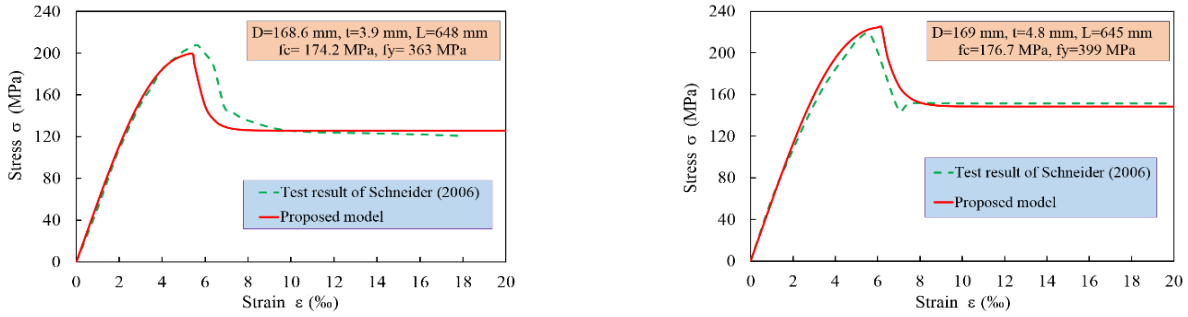

(a) (b)

Fig. 11 Comparison of stress-strain curves between proposed model and test results for columns with steel thicknesses (a) t = 3.9 mm; and (b) t = 4.8 mm

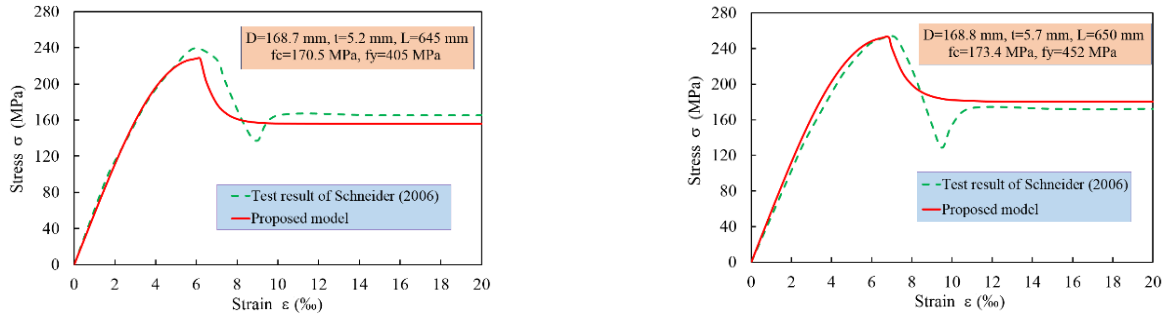

(a) (b)

Fig. 12 Comparison of stress-strain curves between proposed model and test results for columns with steel thicknesses (a) t = 5.2 mm; and (b) t = 5.7 mm

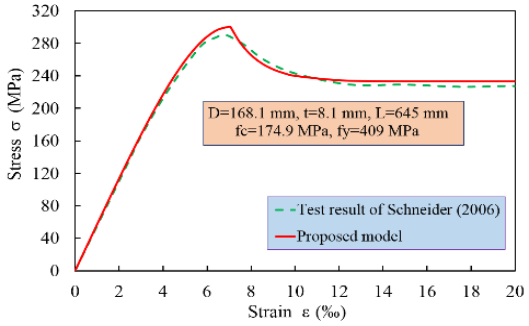

Fig. 13 Comparison of stress-strain curves between proposed model and test results with steel thickness t = 8.1 mm

peak stress and the horizontal plateau after the second peak stress are very well described by the proposed model. The descending parts in predicted curves are found to be steeper with thinner steel tube thicknesses, this observation matches the test results very well. Hence, the descending part of σ-ε curves can be accurately predicted using the proposed model.

It is expected that engineers can easily use this simplified model to predict the stress-strain curves of circular STCC stub columns using UHPC for engineering design.

5. Conclusions

The main objective of this study was an assessment of the performance of circular STCC short columns using UHPC with the cylinder compressive strengths higher than 150 MPa. The following conclusions were drawn within the limitations of the research work in this paper:

- Overall, circular STCC stub columns using UHPC enable better confinement effect which results in higher compressive strength and better ductility compared to ordinary circular UHPC-FSTCs loaded on the entire section.
- To ensure sufficient ductility following the recommendation in Liew *et al*. (2014) and to obtain the significant strength enhancement for circular STCC stub columns using UHPC, the limitation on minimum value of confinement factor ξ should be larger than 0.3 and the D/t ratio should be lower than 30.
- With regard to standard codes, AISC and AIJ underestimates the ultimate loads of circular STCC columns using UHPC by 14.2% and 7.5% on average, respectively; while EC4 overestimates with smaller difference by approximately 4.5% compared to test results. The AIJ code may be preferable to AISC and EC4 because the predictions from AIJ are safer and quite close to measured values.
- EC4 gives better predictions for circular STCC stub columns using UHPC with thicker steel tube walls than those with thinner ones, while for specimens with thinner ones, AISC or AIJ can be used since they provide more accurate predictions compared to test results.
- The predictions of ultimate loads from the seven analytical models are very close to the test results. Thus these models can reliably be used for computing the ultimate loads of circular STCC stub columns using UHPC. Among these models, the model proposed by Sakino *et al*. (2004) is the best predictor.
- A simplified model for stress-strain curve of confined UHPC in circular STCC stub columns was proposed. Comparisons are made between the predicted stress-strain curves and the test results. It was shown that the prediction of both ascending branch and descending branch of stress-strain curves are in good agreement with test results.
- The findings in this study shall establish the basis for the practical application of UHPC in CFSTCs. To gain clearer insights into the behavior of STCC columns using UHPC and to justify or to extend both design codes and previous analytical models of confined concrete in CFSTCs, additional experimental tests should be conducted.

Acknowledgments

The work described in this paper was conducted by An Le Hoang as a part of his Doctoral study under the supervision of Prof. Dr.-Ing. Ekkehard Fehling. The first author would like to acknowledge Vietnamese Government, DAAD for the support of his full PhD scholarship and Institute of Structural Engineering – University of Kassel for their financial support of the experimental project titled "Behavior of circular steel tube confined UHPC and UHPFRC columns".

References

American Institute of Steel Construction (ANSI/AISC 360-10) (2010), Specification for Structural Steel Buildings; An American National Standard.

Architectural Institute of Japan (AIJ) (2001), Recommendation for design and construction of concrete filled steel tubular structures; Japan. [In Japanese]

Binici, B. (2005), "An analytical model for stress-strain behavior of confined concrete", *Eng. Struct.*, **27**(7), 1040-1051.

Chu, K. (2014), "Axial load behaviour of steel tube columns in-filled with various high-performance concretes", Master Thesis; Ryerson University, Toronto, ON, Canada.

De Oliveira, W.L.A., De Nardin, S., De Cresce El Debs, A.L.H. and El Debs, M.K. (2009), "Influence of concrete strength and length/diameter on the axial capacity of CFT columns", *J. Constr. Steel Res.*, **65**(12), 2103-2110.

De Oliveira, W.L.A., De Nardin, S., De Cresce El Debs, A.L.H. and El Debs, M.K. (2010), "Evaluation of passive confinement in CFT columns", *J. Constr. Steel Res.*, **66**(4), 487-495.

Eurocode 4 (2004), Design of composite steel and concrete structures; Part 1.1, General rules and rules for Building, BS EN 1994-1-1; British Standards Institution, London, UK.

Fam, A., Qie, F.S. and Rizkalla, S. (2004), "Concrete-filled steel tubes subjected to axial compression and lateral cyclic loads", *J. Struct. Eng., ASCE*, **130**(4), 631-640.

Fehling, E., Schmidt, M., Walraven, J., Leutbecher, T. and Fröhlich, S. (2014), Ultra-High Performance Concrete: Fundamental – Design – Example; Wilhelm Ernst & Sohn, Verlag für Architektur und technische Wissenschaften GmbH & Co. KG, Rotherstraße 21, 10245 Berlin, Germany.

Guler, S., Aydogan, M. and Copur, A. (2013), *Axial Capacity and Ductility of Circular UHPC-filled Steel Tube Columns*, Magazine of Concrete Research, February.

Han, L.H., Yao, G.H., Chen, Z.P. and Yu, Q. (2005), "Experimental behavior of steel tube confined concrete (STCC) columns", *Steel Compos. Struct., Int. J.*, **5**(6), 459-84.

Han, L.H., Li, W. and Bjorhovde, R. (2014), "Development and advanced applications of concrete-filled steel tubular (CFST) structures: members", *J. Constr. Steel Res.*, **100**, 211-228.

Hatzigeorgiou, G.D. (2008), "Numerical model for the behavior and capacity of circular CFT columns, Part I: Theory", *Eng. Struct.*, **30**(6), 1573-1578.

Johansson, M. (2002), "The efficiency of passive confinement in CFT columns", *Steel Compos. Struct., Int. J.*, **2**(5), 379-396.

Johansson, M. and Gylltoft, K. (2001), "Structural behavior of slender circular steel-concrete composite columns under various means of load application", *Steel Compos. Struct., Int. J.*, **1**(4), 393-410.

Johansson, M. and Gylltoft, K. (2002), "Mechanical behavior of circular steel-concrete composite stub columns", *J. Struct Eng.*, ASCE, **128**(8), 1073-1081.

Liang, Q.Q. and Fragomeni, S. (2009), "Nonlinear analysis of circular concrete-filled steel tubular short columns under axial loading", *J. Constr. Steel Res.*, **65**(12), 2186-2196.

Liew, J.Y.R. and Xiong, D.X. (2010), "Experimental investigation on tubular columns infilled with ultra-high strength concrete",

Tubular Structures XIII, The University of Hong Kong, pp. 637-645.

Liew, J.Y.R. and Xiong, D.X. (2012), "Ultra-high strength concrete filled composite columns for multi-storey building construction", *Adv. Struct. Eng.*, **15**(9), 1487-1503.

Liew, J.Y.R. and Xiong, M.X. (2015), "Design Guide For Concrete Filled Tubular Members With High Strength Materials to Eurocode 4", *Research Publishing*, Blk 12 Lorong Bakar Batu, 349568 Singapore.

Liew, J.Y.R., Xiong, M.X. and Xiong, D.X. (2014), "Design of high strength concrete filled tubular columns for tall buildings", *Int. J. High-Rise Building*, **3**(3), 215-221.

O'Shea, M.D. and Bridge, R.Q. (1997a), "Test on circular thin-walled steel tubes filled with medium and high strength concrete", Department of Civil Engineering Research Report No. R755; The University of Sydney, Sydney, Australia.

O'Shea, M.D. and Bridge, R.Q. (1997b), "Test on circular thin-walled steel tubes filled with very high strength concrete", Department of Civil Engineering Research Report No. R754; The University of Sydney, Sydney, Australia.

O'Shea, M.D. and Bridge, R.Q. (2000), "Design of circular thin-walled concrete filled steel tubes", *J. Struct Eng.*, ASCE, **126**(11), 1295-1303.

Orito, Y., Sato, Y., Tanaka, N. and Watanabe, K. (1987), "Study on the unbonded steel tube concrete structure", *Proceedings of Engineering Foundation Conference on Composite Constructions*, Henniker, NH, USA, June, pp. 786-804.

Sakino, K., Tomii, M. and Watanabe, K. (1985), "Sustaining load capacity of plain concrete stub columns confined by circular steel tubes", *Proceedings of the International Specialty Conference on Concrete-Filled Steel Tubular Structures*, *ASCCS*, Harbin, China, August, pp. 112-118.

Sakino, K., Nakahara, H. Morino, S. and Nishiyama, I. (2004), "Behavior of centrally loaded concrete-filled steel-tube short columns", *J. Struct. Eng.*, *ASCE*, **130**(2), 180-188.

Samani, A.K. and Altard, M.M. (2012), "A stress-strain model for uniaxial and confined concrete under compression", *Eng. Struct.*, **41**, 335-349.

Schmidt, M. and Fehling, E. (2005), "Ultra-high-performance concrete: research, development and application in europe", *ACI Struct. J. Special Publication*, **228**, 51-78.

Schneider, S.P. (1998), "Axially loaded concrete-filled steel tubes", *J. Struct Eng.*, *ASCE*, **124**(10), 1125-1138.

Schneider, H. (2006), "Zum tragverhalten kurzer, umschnürter, kreisförmiger, druckglieder aus ungefasertem UHFB", Ph.D. Dissertation; University of Leipzig, Leipzig, Germany.

Susantha, K.A.S., Ge, H. and Usami, T. (2001), "Uniaxial stress-strain relationship of concrete confined by various shaped steel tubes", *Eng. Struct.*, **23**(10), 1331-1347.

Tao, Z., Wang, Z.B. and Yu, Q. (2013), "Finite element modelling of concrete filled steel stub columns under axial compression", *J. Constr. Steel Res.*, **89**, 121-131.

Tomii, M., Sakino, K., Watanabe, K. and Xiao, Y. (1985), "Lateral load capacity of reinforced concrete short columns confined by steel tube", *Proceedings of the International Specialty Conference on Concrete Filled Steel Tubular Structures*, *ASCCS*, Harbin, China, August, pp. 19-26.

Tue, N.V., Schneider, H., Simsch, G. and Schmidt, D. (2004a), "Bearing capacity of stub columns made of NSC, HSC and UHPC confined by a steel tube", *Proceedings of the 1st International Symposium on Ultra High Performance Concrete*, Kassel, Germany, March, pp. 339-350.

Tue, N.V., Küchler, M., Schenck, G. and Jürgen, R. (2004b), "Application of UHPC filled tubes in buildings and bridges", *Proceedings of the 1st International Symposium on Ultra High Performance Concrete*, Kassel, Germany, March, pp. 807-817.

Xiong, D.X. (2012), "Structural behaviour of concrete filled steel tube with high strength materials", Ph.D. Dissertation; National University of Singapore, Singapore.

Yan, P.Y. and Feng, J.W. (2008), "Mechanical behavior of UHPC and UHPC filled steel tubular stub columns", *Proceedings of the 2nd International Symposium on Ultra High Performance Concrete*, Kassel, Germany, March, pp. 355-362.

Yu, Q., Tao, Z., Liu, W. and Chen, Z.B. (2010), "Analysis and calculations of steel tube confined concrete (STCC) stub columns", *J. Constr. Steel Res.*, **66**(1), 53-64.

Zhong, S.T. and Miao, R.Y. (1988), "Stress-strain relationship and strength of concrete filled tubes", *Proceedings of Engineering Foundation Conference on Composite Constructions*, Henniker, NH, USA, June, pp. 773-785.

DL